Nanoscale optical tomography using volume-scanning near-field microscopy

Jin Sun, John C. Schotland, Rainer Hillenbrand, and P. Scott Carney

Citation: Appl. Phys. Lett. **95**, 121108 (2009); doi: 10.1063/1.3224177
View online: http://dx.doi.org/10.1063/1.3224177
View Table of Contents: http://apl.aip.org/resource/1/APPLAB/v95/i12
Published by the American Institute of Physics.

Nanoscale optical tomography using volume-scanning near-field microscopy

Jin Sun,[1] John C. Schotland,[2] Rainer Hillenbrand,[3] and P. Scott Carney[4,a)]
[1]*Department of Electrical and Computer Engineering, University of Illinois, Urbana, Illinois 61801, USA*
[2]*Department of Bioengineering and Graduate Group in Applied Mathematics and Computational Science, University of Pennsylvania, Philadelphia, Pennsylvania 19104, USA*
[3]*Nanooptics Laboratory, CIC nanoGUNE Consolider, 20018 Donostia-San Sebastian and IKERBASQUE, Basque Foundation for Science, Spain*
[4]*Department of Electrical and Computer Engineering and The Coordinated Science Laboratory, University of Illinois, Urbana, Illinois 61801, USA*

(Received 16 April 2009; accepted 18 August 2009; published online 23 September 2009)

The relationship between sample structure and data in volume-scanning backscattering mode near-field optical microscopy is investigated. It is shown that the three-dimensional structure of a dielectric sample is encoded in the phase and amplitude of the scattered field and that an approximate reconstruction of the sample structure may be obtained. © *2009 American Institute of Physics*. [doi:10.1063/1.3224177]

Near-field scanning optical microscopy (NSOM)[1–7] is a method for nanoscale optical imaging that achieves subwavelength resolution by detecting the evanescent wave fields accessible in the near-zone of a scattering object. In conventional NSOM, the intensity of the optical field in a plane above a three-dimensional sample is interpreted as a two-dimensional image of the sample. This interpretation is known to be problematic since the three-dimensional structure of the medium is not uniquely determined by the two-dimensional intensity map which constitutes the NSOM image. Means to interpret NSOM images have been developed,[8,9] including the solution of a three-dimensional near-field inverse scattering problem.[10–18] The resulting methods are known as near-field optical tomography (NFOT). NFOT experiments require the acquisition of multiple complete NSOM data sets for varying directions of illumination or observation of the field.[17,18] This requirement presents serious obstacles to experimental implementation, except in special cases such as the imaging of two-dimensional samples.[11]

The results of NSOM experiments in which the probe is scanned over a three-dimensional volume outside the sample[19,20] suggest that the three-dimensional structure of the sample may be unambiguously determined. That is, the so-called approach curves, or measured intensity as a function of height above the sample, are seen in Ref. 19 to vary depending on the depth of subsurface features of the sample.[20,21] Such an experiment is attractive because, though multiple NSOM data sets must be acquired (at a variety of scan heights above the sample), the directions of the far-field illumination and observation may be held fixed. The independence of data acquired at multiple heights is somewhat unexpected.

In illumination or collection mode NSOM, data from different planes are related by propagation or backpropagation of the scattered field.[22] Consider specifically collection mode NSOM; the illuminating source is fixed while the scattered field is collected on a plane by scanning the probe. The field that would be detected on a plane farther from the sample is completely determined by knowledge of the measured field through the standard Kirchhoff–Helmholtz integral theorem which holds in the near-field.[23] Data acquired by fixing the detector and scanning the illuminating probe in a plane may transformed into data obtained by scanning the illumination in a different plane by similar integral transforms. In the backscattered mode NSOM discussed in this letter, however, data sets collected with the probe at a variety of distances from the sample are *independent*. The illumination and detection are varied simultaneously. While the scattered field may be propagated from one plane to the next, moving the probe to the next plane also changes the scattered field because the illumination changes. The data collected by scanning the probe on one plane do not predict the data collected by scanning on a different plane and so the data are independent. Thus three-dimensional reconstruction of the sample may be obtained by a method, which we refer to as volume-scanning NFOT (vNFOT).

We begin by considering an experiment in which a weakly scattering sample with dielectric susceptibility η is placed in vacuum above a half-space with constant refractive index n. An NSOM probe tip in the near-zone of the sample serves as a point source of illumination. The backscattered field is collected by the tip, which is scanned in a three-dimensional volume above the sample, as shown in Fig. 1. It is important to note that volume-scanning near-field tomography leads to considerable experimental simplicity compared to other variants of NFOT. For instance, collection-mode NFOT requires scanning of both the near-field probe and the source of illumination.[17]

The incident field produced by an electric dipole $\mathbf{p}_1$, located at the tip position $\mathbf{r}_t=(\boldsymbol{\rho}_t, z_t)$, is given by the expression

$$\mathbf{E}_i(\mathbf{r}) = k_0^2 \mathbf{G}(\mathbf{r}, \mathbf{r}_t) \cdot \mathbf{p}_1, \tag{1}$$

where k_0 is the free-space wave number and $\mathbf{G}$ is the half-space Green's tensor. The Green's tensor is given by the plane wave representation

a)Electronic mail: carney@uiuc.edu.

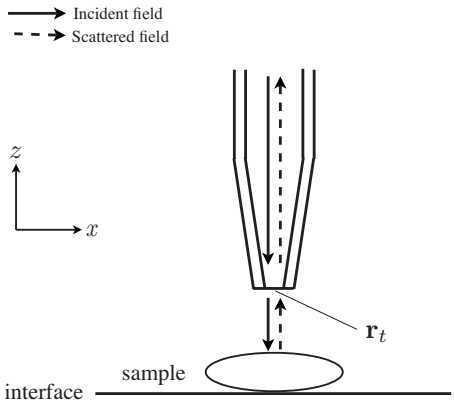

FIG. 1. Illustrating the vNVOT experiment.

$$\mathbf{G}(\mathbf{r},\mathbf{r}') = \frac{i}{2\pi}\int d^2q\mathbf{g}(z,z';\mathbf{q})\exp[i\mathbf{q}\cdot(\boldsymbol{\rho}-\boldsymbol{\rho}')], \tag{2}$$

where $\mathbf{r}=(\boldsymbol{\rho},z)$, $\mathbf{r}'=(\boldsymbol{\rho},'z')$, and the quantity $\mathbf{g}(z,z';\mathbf{q})$ is given in Ref. 18.

The field scattered from the sample, within the accuracy of the first Born approximation,[22] is given by

$$\mathbf{E}_s(\mathbf{r}) = k_0^2\int d^3r'\mathbf{G}(\mathbf{r},\mathbf{r}')\mathbf{E}_i(\mathbf{r}')\,\eta(\mathbf{r}'). \tag{3}$$

The measured signal consists of a component of the scattered field in the $\mathbf{p}_2$ direction and is denoted $S=\mathbf{E}_s\cdot\mathbf{p}_2$. Substituting Eq. (1) into Eq. (3), we find that the signal is given by

$$S(\mathbf{r}_t) = k_0^4\int d^3r\mathbf{p}_2\cdot\mathbf{G}(\mathbf{r}_t,\mathbf{r})\mathbf{G}(\mathbf{r},\mathbf{r}_t)\cdot\mathbf{p}_1\,\eta(\mathbf{r}). \tag{4}$$

Equation (4) defines the forward model for vNFOT.

In the above analysis, the tip is modeled as a pointlike dipole when used as a source of illumination and a pointlike polarized detector when collecting the backscattered field, as is often encountered in the literature.[24] It is noted that this assumption is neither restrictive nor exclusive. Other models, such as an extended dipole model, magnetic dipole model, or electric monopole model,[24–27] may be used in a strictly similar manner, without altering the basic theory.

The inverse problem of vNFOT is to recover the susceptibility η from volumetric measurements of the backscattered field. To proceed, we define the data function $\Phi(\mathbf{q}_t,z_t)$ to be the two-dimensional lattice Fourier transform of $S(\mathbf{r}_t)$ in the plane $z=z_t$:

$$\Phi(\mathbf{q}_t,z_t) = h^2\sum_{\boldsymbol{\rho}} S(\boldsymbol{\rho},z_t)e^{-i\mathbf{q}\cdot\boldsymbol{\rho}}, \tag{5}$$

where the sum over $\boldsymbol{\rho}$ is carried out over all lattice vectors on a two-dimensional square lattice with lattice spacing h and $\mathbf{q}$ belongs to the first Brillouin zone (FBZ) of the lattice. Substituting Eq. (4) into Eq. (5), making use of Eq. (2) and the identity

$$\sum_{\boldsymbol{\rho}} e^{i\mathbf{q}\cdot\boldsymbol{\rho}} = \left(\frac{2\pi}{h}\right)^2\sum_{\mathbf{q}'}\delta(\mathbf{q}-\mathbf{q}'), \tag{6}$$

where the sum over $\mathbf{q}'$ is carried out over the reciprocal lattice, we find that the data function becomes

$$\Phi(\mathbf{q}_t,z_t) = -k_0^4\sum_{\mathbf{q}'}\int dz\int d^2q\mathbf{p}_2\cdot\mathbf{g}(z_t,z,\mathbf{q}) \times\mathbf{g}(z,z_t,\mathbf{q}-\mathbf{q}_t-\mathbf{q}')\cdot\mathbf{p}_1\tilde{\eta}(\mathbf{q}_t+\mathbf{q}',z), \tag{7}$$

where $\tilde{\eta}$ is the transverse Fourier transform of the sample function $\eta(\mathbf{r})=\eta(\boldsymbol{\rho},z)$ defined by

$$\tilde{\eta}(\mathbf{q},z) = \int d^2\rho\,\eta(\boldsymbol{\rho},z)e^{-i\mathbf{q}\cdot\boldsymbol{\rho}}. \tag{8}$$

Assuming that the sample function is transversely bandlimited to the FBZ, the sum over the reciprocal lattice vectors in Eq. (8) may be truncated, leaving only the $\mathbf{q}'=0$ term. Thus, the data function becomes

$$\Phi(\mathbf{q}_t,z_t) = \int dzK(z_t,z;\mathbf{q}_t)\tilde{\eta}(\mathbf{q}_t,z), \tag{9}$$

where the kernel K is given by the expression

$$K(z_t,z;\mathbf{q}_t) = -k_0^4\int d^2q\mathbf{p}_2\cdot\mathbf{g}(z_t,z,\mathbf{q})\mathbf{g}(z,z_t,\mathbf{q}-\mathbf{q}_t)\cdot\mathbf{p}_1. \tag{10}$$

For fixed $\mathbf{q}_t$, Eq. (9) defines a one-dimensional integral equation whose solution is given by

$$\tilde{\eta}^+(\mathbf{q}_t,z) = \sum_{z_t} K^+(z,z_t,\mathbf{q}_t)\Phi(\mathbf{q}_t,z_t), \tag{11}$$

where K^+ is the pseudoinverse of K. Note that the computation of K^+ requires regularization in order to obtain a stable solution to the inverse problem.[28] The final step of the reconstruction of η is to compute the inverse Fourier transform of $\tilde{\eta}^+(\mathbf{q}_t,z)$ for each z.

Numerical simulations were conducted to demonstrate the proposed method. We consider an object consisting of three point scatterers located in the $y=0$ plane above the interface is assumed, as is shown in Fig. 2(a). The index of refraction of the lower half space is set to be 1.5. A tip is initially located in the $z_0=0.32\lambda$ plane, where $\lambda=2\pi/k_0$ is the free-space wavelength. The tip is assumed to be strongly coupled to the z-component of the field at the tip so that $\mathbf{p}_1=\mathbf{p}_2=p_0\hat{z}$. This choice does not significantly affect the result. The tip is scanned in the z-direction from $z=0.32\lambda$ to $z=0.63\lambda$, with a spacing of 0.008λ. In the transverse direction the tip is scanned with a lattice spacing of 0.063λ. Forward scattering data are calculated from Eq. (4) and white Gaussian noise is added at two different levels with a signal-to-noise ratio of 125 and 75 dB.

Reconstructed images of the sample are shown in Fig. 2(b). It can be seen that we obtain subwavelength resolution in the transverse direction and a depth resolution of $\sim\lambda/12$. The depth resolution is highest close to the tip and falls off with distance into the sample. Note that the transverse resolution is also depth dependent, due to the exponential decay of evanescent waves. The reconstructions are relatively sensitive to noise, consistent with the ill posedness of the inverse scattering problem for wave fields with evanescent components. Regularization commensurate with noise levels results in the resolution of the reconstruction being determined also by the noise. Regularization disproportionately dampens the contribution of high spatial-frequency components of the reconstructions.

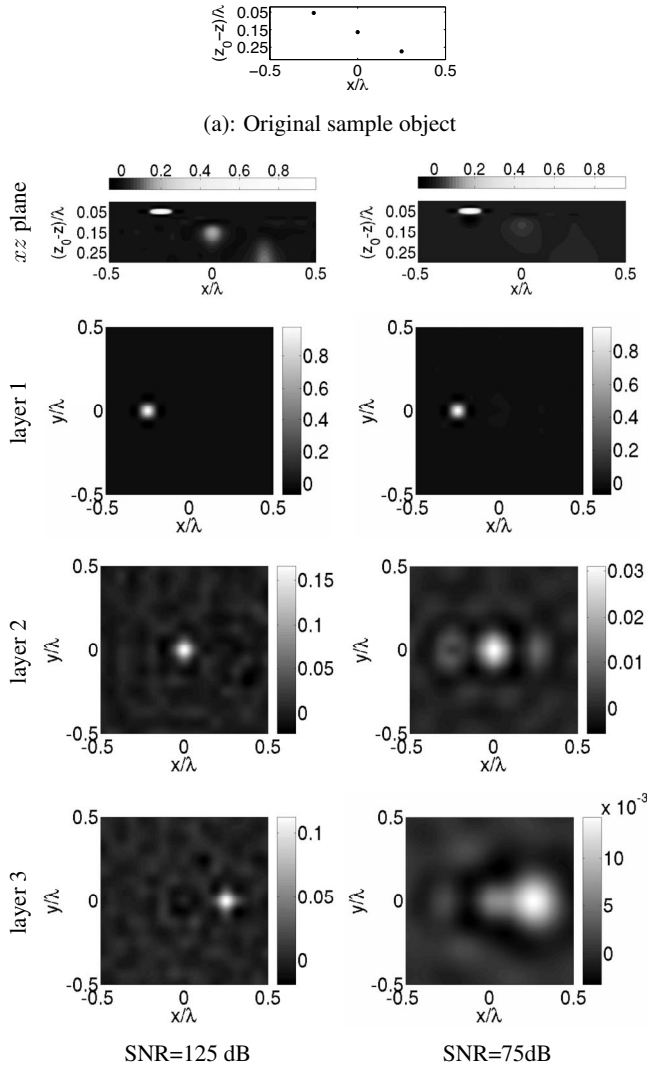

(a): Original sample object

(b): Reconstructions under different levels of SNR

FIG. 2. Reconstructed images in vNFOT. (a) The sample. (b) Reconstructions in the *xz* plane and three transverse layers parallel to the *xy* plane in which the three point scatterers are located. Each image is normalized to its own maximum.

In conclusion, we have presented an analysis of the inverse scattering problem for vNFOT. The proposed method may provide a simpler and more robust means to perform NFOT and has potential applications to three-dimensional imaging of subsurface nanostructures.

The work of P.S.C. was supported in part by U.S. Air Force MURI Grant No. F49620-03-10379 and in part by the National Science Foundation under CAREER Award Grant No. 0239265. J.C.S. acknowledges support by the NSF under the Grant No. DMR 0425780 and by the USAFOSR under the Grant No. FA9550-07-1-0096.

[1]E. Synge, Philos. Mag. **6**, 356 (1928).
[2]C. Girard and A. Dereux, Rep. Prog. Phys. **59**, 657 (1996).
[3]E. Ash and G. Nicholls, Nature (London) **237**, 510 (1972).
[4]A. Lewis, M. Isaacson, A. Harootunian, and A. Muray, Ultramicroscopy **13**, 227 (1984).
[5]D. W. Pohl, W. Denk, and M. Lanz, Appl. Phys. Lett. **44**, 651 (1984).
[6]E. Betzig and J. K. Trautman, Science **257**, 189 (1992).
[7]L. Novotny, D. W. Pohl, and B. Hecht, Ultramicroscopy **61**, 1 (1995).
[8]R. Carminati and J.-J. Greffet, J. Opt. Soc. Am. A Opt. Image Sci. Vis **12**, 2716 (1995).
[9]R. Carminati and J.-J. Greffet, Ultramicroscopy **61**, 11 (1995).
[10]P. S. Carney and J. C. Schotland, Appl. Phys. Lett. **77**, 2798 (2000).
[11]P. S. Carney, R. A. Frazin, S. I. Bozhevolnyi, V. S. Volkov, A. Boltasseva, and J. C. Schotland, Phys. Rev. Lett. **92**, 163903 (2004).
[12]P. C. Chaumet, K. Belkebir, and A. Sentenac, Opt. Lett. **29**, 2740 (2004).
[13]K. Belkebir, P. C. Chaumet, and A. Sentenac, J. Opt. Soc. Am. A Opt. Image Sci. Vis **22**, 1889 (2005).
[14]A. Sentenac, P. C. Chaumet, and K. Belkebir, Phys. Rev. Lett. **97**, 243901 (2006).
[15]G. Y. Panasyuk, V. A. Markel, P. S. Carney, and J. C. Schotland, Appl. Phys. Lett. **89**, 221116 (2006).
[16]G. Bao and P. Li, Opt. Lett. **32**, 1465 (2007).
[17]J. Sun, J. C. Schotland, and P. S. Carney, IEEE J. Sel. Top. Quantum Electron. **12**, 1072 (2006).
[18]J. Sun, P. S. Carney, and J. C. Schotland, J. Appl. Phys. **102**, 103103 (2007).
[19]R. Hillenbrand and F. Keilmann, Phys. Rev. Lett. **85**, 3029 (2000).
[20]T. Taubner, F. Keilmann, and R. Hillenbrand, Opt. Express **13**, 8893 (2005).
[21]N. Anderson, P. Anger, A. Hartschuh, and L. Novotny, Nano Lett. **6**, 744 (2006).
[22]M. Born and E. Wolf, *Principles of Optics*, 6th ed. (Pergamon, Oxford, 1980).
[23]M. D. Karabacak, K. L. Ekinci, S. B. Ippolito, C. H. Gan, G. J. Gbur, M. S. Ünlü, B. B. Goldberg, and P. S. Carney, Opt. Lett. **32**, 1881 (2007).
[24]L. Novotny and B. Hecht, *Principles of Nano-Optics*, 1st ed. (Cambridge University Press, Cambridge, 2006).
[25]H. A. Bethe, Phys. Rev. **66**, 163 (1944).
[26]C. J. Bouwkamp, Philips. Res. Rep. **5**, 401 (1950).
[27]A. Cvitkovic, N. Ocelic, and R. Hillenbrand, Opt. Express **15**, 8550 (2007).
[28]P. S. Carney and J. C. Schotland, *Inside Out: Inverse Problems*, edited by Gunther Uhlman (Cambridge University Press, Cambridge, 2003), pp. 131–166.